Chapter 33
Numerical Studies on the Heat Insulation and Smoke Control Effect of Water Mist Screen Under Longitudinal Ventilation in Bifurcated Tunnel

Yujie Lan, Xinyi Liu, Haifeng Chen, Xineng Yan, Shanxin Zhou, Xiaosong Li, and Longfei Chen

Abstract As the complex structure, the situation of fire accident of a bifurcated tunnel will be more severe than that of a long-straight tunnel. It is of practical significance to research the control effect of the water mist screens in the bifurcated tunnel fire. In this paper, a 1/10 scale bifurcated tunnel model is established based on FDS to study the heat insulation and smoke control effect of water mist screen under the action of longitudinal ventilation when a fire occurs at the fork. The results indicated that: The coupling of longitudinal ventilation and water mist has the most significant inhibition effect on ceiling temperature and ceiling CO concentration in the upstream area of main tunnel, the larger wind speed results in better heat insulation and smoke control effect in the upstream area of main tunnel. Overall, the more the number of water mist nozzle rows or the smaller the particle size, the better the control effect on the ceiling temperature and ceiling CO concentration of the main and branch tunnel. In addition, compared with the main road, the water mist screen section of branch tunnel has the limited ability to block the smoke diffusion.

Keywords Bifurcated tunnel · Water mist screen · Longitudinal ventilation · Temperature · CO concentration

Y. Lan · X. Liu · H. Chen · X. Yan · S. Zhou · X. Li · L. Chen (✉)
Department of Fire Protection Engineering, Southwest Jiaotong University, Chengdu 610031, China
e-mail: longfeichen@swjtu.edu.cn

X. Li
Department of Security, Sichuan University, Chengdu 610065, China

S. Li (ed.), *Computational and Experimental Simulations in Engineering*,
Mechanisms and Machine Science 143,
https://doi.org/10.1007/978-3-031-42515-8_33

33.1 Introduction

The tunnel structure has long-narrow and closed characteristics, fires can easily cause congestion and vehicle collisions, resulting in very serious consequences. Compared with the traditional water-based fire extinguishing system, the water mist system is atomized into small-sized droplets by spraying water through a special structure nozzle under a certain pressure, which can fill the space to achieve the effects of cooling, suffocation, and blocking radiant heat. At the same time, it can reduce impact on circuits, flammable and explosive materials, etc. Moreover, the water mist system has the advantages of fast heat absorption, no pollution and low water consumption. Therefore, the application of water mist system has attracted the attention of many scholars [1, 2].

The direct action on fire source with water system has been studied extensively by scholars. Chen et al. [3] conducted a 1:10 reduced-scale study referring to the experiment of Siemens and proposed that the establishment of a coupling system of water mist and ventilation could significantly improve the efficiency of fire extinguishing. Under longitudinal ventilation, the interaction between water mist and smoke has been carried out in a numerical simulation (Blanchard et al. [4]), and verified the effectiveness of water mist to absorb heat and radiation. The experimental results of Li et al. [5] in a small-scale tunnel showed that with longitudinal ventilation, water mist can effectively suppress the n-heptane pool fire, and the cooling effect was enhanced with the ventilation velocity. The experiments by Wang et al. [6] showed that the maximum smoke temperature decreased with the increase of the water mist flow, and the exponential equation of the longitudinal smoke temperature distribution was modified. Yang et al. [7] studied the variation of particle size on smoke migration with longitudinal velocity in road tunnel and indicated that there was an optimal water mist fire extinguishing particle size. Li et al. [8] found that the fire extinguishing efficiency of fixed fire extinguishing system can be improved to a certain extent by longitudinal ventilation, and the ventilation system should operate earlier than FFFS. Liu et al. [9] investigated the combined effect of a water mist system and longitudinal ventilation, the results showed that the internal tunnel temperature decreased significantly under longitudinal airflow, especially in the upstream area and near fire source. Magdolenova [10] carried out a numerical simulation of a 1/3 scale model and pointed out that the system with double-row nozzle arrangement was more stable.

There are relatively few studies on the situation that no direct contact between the fire source and the water mist. Sun et al. [11] indicated that when the wind speed reached the critical value, the water system will have less role in preventing smoke diffusion would be reduced, although the temperature decrease phenomenon in the downstream area still existed. A new system with simultaneous water mist screen and transverse ventilation system (WMSTV system) is proposed by Liang et al. [12], they found that the visibility in the closed area between the two water mist screens was low, but the temperature at 2 m above the ground was relatively low and would be suitable for personnel evacuation. Wang et al. [13] conducted

a numerical simulation study on the coupling of longitudinal ventilation and water mist. Results showed that the downstream temperature decreased with the increase in the length of water mist zone, while the temperature did not change significantly with the water pressure. Li et al. [14] revealed that the water mist segment system should not be used in combination with longitudinal ventilation. In the study of Mehaddi et al. [15], they concluded that the smoke flow could not be prevented by the water curtain, but it could achieve greater radiation attenuation. Fan et al. [16] conducted a full-scale experiment in the railway tunnel rescue station, and the results showed that longitudinal ventilation could help enhance the visibility and reduce temperature. In the area covered by water mist, the dimensionless maximum temperature rise under longitudinal ventilation was lower than that without it.

Based on the above analysis, the research of water mist screen in tunnels is mainly based on long and straight tunnels. There is no specific research result on the application of water mist screen to bifurcated tunnels. Compared with the long straight tunnel, the bifurcated tunnel is more complex and traffic accidents are relatively frequent at the fork. This paper mainly studies the smoke temperature and the CO concentration distributions in bifurcated tunnel fire by changing heat release rate of fire source, longitudinal ventilation velocity, number of row of water mist nozzle and particle size of water mist.

33.2 Numerical Simulation

33.2.1 Numerical Model

Based on the similarity criterion [17, 18], a 1:10 bifurcation tunnel numerical model is established in this study. In Fig. 33.1, the dimension of the main tunnel is 10 m (length) × 1.5 m (width) × 0.6 m (height), and the branch is 5 m (length) × 1 m (width) × 0.6 m (height). The angle between the main tunnel and the branch tunnel is 45°. A series of thermocouples and carbon monoxide measuring points are arranged longitudinally along the center of the tunnel ceiling. A fire source with a size of 0.2 m × 0.2 m × 0.1 m is set at the center of the main tunnel, and propane is used as fuel. The longitudinal ventilation is set on the left side of the main tunnel. The main tunnel takes the fire source center as the origin O_A and the branch tunnel takes the fork center as the origin O_B. The tunnel is provided with three sections of water mist screen, each section has three rows of water mist nozzles with an interval of 0.5 m. The upstream water mist screen section of the main tunnel is set at −2 to −3 m, the downstream water mist screen section of the main tunnel is set at 2–3 m, and the water mist screen of the branch is set at 1.5–2.5 m. The row of water mist closest to the fire source is defined as the first row, and so on. During the process of simulation, longitudinal ventilation is activated firstly, the same number of row of water mist nozzle are activated at the same time in the main road and branch at 150 s, and the water mist system stops working at 300 s.

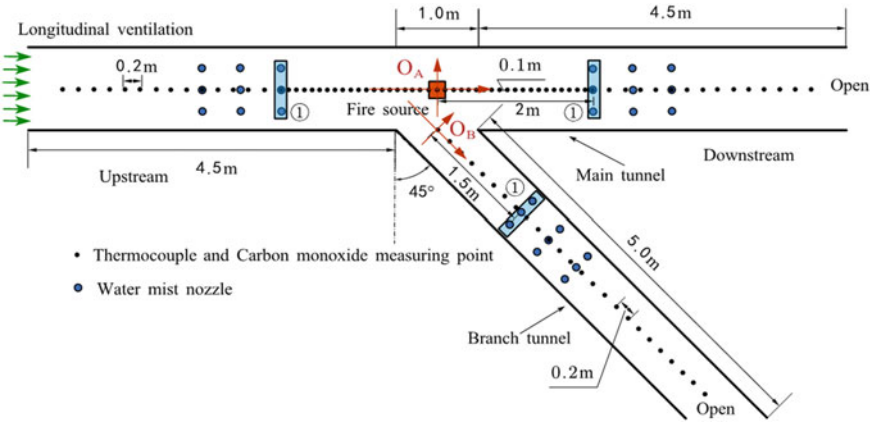

Fig. 33.1 Top view diagram of numerical model

33.2.2 Simulation Conditions

Table 33.1 shows the details of the simulation conditions, considering the heat release rates of fire source (HRR), the longitudinal ventilation velocity (v), the number of row of water mist nozzle and the particle size of water mist (D) as variables. A total of 60 working conditions are simulated.

Table 33.1 Summary of the simulation conditions

No	HRR (kW)	Longitudinal ventilation velocity (m/s)	Number of row of water mist nozzle	Working pressure (bar)	Water mist nozzle flow (L/min)	Particle size of water mist (μm)	Spray angle (°)
1–9	31.62	0.3	1, 2, 3	2	1.2	50	60
10–18		0.4				100	
19–27		0.5				200	
28–36	63.25	0.3	1, 2, 3			50	
37–45		0.4				100	
46–54		0.5				200	
55–60	31.62 63.25	0.3, 0.4, 0.5	0	–	–	–	–

33.2.3 Grid Independence Analysis

The setting basis of grid size used in numerical simulation of this study is as follow [19]:

$$D^* = \left(\frac{HRR}{\rho_\infty c_p T_\infty \sqrt{g}}\right)^{\frac{2}{5}} \tag{33.1}$$

$$4 < \frac{D^*}{\delta x} < 16 \tag{33.2}$$

where D^* is the characteristic diameter of fire source, c_p is the specific heat capacity of ambient air (kJ/(kg K)), T_∞ is the ambient air temperature (K), δ_x is the grid size, ρ_∞ is the ambient air density (kg/m^3).

When the heat release rate of fire source is 31.62 kW, the calculated grid size is between 0.01 and 0.06 m. When the heat release rate of fire source is 63.25 kW, the calculated grid size is between 0.02 and 0.08 m. As shown in Fig. 33.2, the grid sizes of 0.04, 0.05 and 0.06 m are selected for temperature distribution analysis beneath the tunnel ceiling. Taking the accuracy and calculation time into consideration, a multi-grid method is used for numerical simulation, i.e., the grid size within 1 m^2 area of the fire source is 0.025 m × 0.025 m × 0.025 m, and the grid size in other areas is 0.05 m × 0.05 m × 0.05 m.

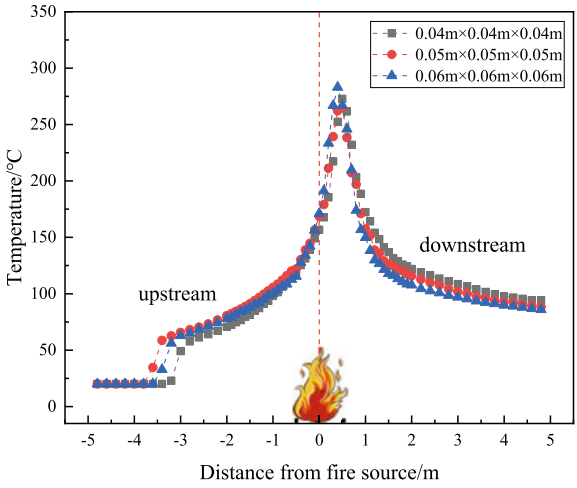

Fig. 33.2 Grid adaptability curve

33.3 Results and Discussions

33.3.1 The Heat Insulation and Smoke Control Effect of the Main Tunnel

33.3.1.1 Temperature Distribution

Figure 33.3 shows the ceiling temperature variation curves on both sides of the water mist screen section in the main tunnel (i.e., at the positions of ±1 and ±4 m away from the fire source). It shows that the water mist nozzles are activated at 150 s and reach stability at about 200 s. After the water mist is sprayed into the fire scene, the droplets evaporate rapidly, which has a strong effect of gasification and cooling. The effect of different number of water mist nozzle rows on the upstream area near the fire source is not obvious in Fig. 33.3a. At 4 m upstream from the fire source (i.e., the outside area of the water mist screen section), the initial ceiling temperature is low due to the influence of longitudinal ventilation. After activating the water mist system, the ceiling temperature drops sharply to ambient temperature, and the cooling effect reaches the best under all the different number of water mist nozzle rows. Due to the existence of water mist screen, the heat transfer at 1 m upstream from the fire source (i.e., the area near the fire source) is inhibited. For the downstream area, the cooling effect of water mist screen section is significant at 4 m downstream from the fire source. When the 3 rows of water mist nozzles come into play, the ceiling temperature at 4 m downstream rapidly decreases to close to the ambient temperature. Increasing the number of water mist nozzle rows is equivalent to increasing the number of droplets, which has a better cooling effect, seen in Fig. 33.3b, d. The ceiling temperature at 1 m downstream from the fire also increases slightly, which is similar with the result of 1 m upstream from the fire.

Figure 33.4 shows the ceiling temperature variation along the main tunnel with different number of nozzle rows activated. It can be observed that, the coupling effect of longitudinal ventilation and water mist has a significant influence on the ceiling temperature in the upstream area. The increase of wind speed inhibits the smoke diffusion in the upstream area. For the same wind speed, no matter how many rows of water mist nozzles act, the ceiling temperature drops to ambient temperature at 2 m upstream away from the fire source. As the wind speed and the number of water mist nozzle rows increase, the sharp drop point of ceiling temperature is closer to the center of the fire source. The ceiling temperature variation of the downstream area is basically consistent with that of the upstream area. The wind speed reduces the maximum ceiling temperature. For the same wind speed, the ceiling temperature decreases obviously after the water mist nozzles are activated. The more the number of water mist nozzle rows is, the greater the reduction of ceiling temperature. The coupling effect of longitudinal ventilation and water mist on the ceiling temperature in the downstream area is not obvious.

In order to study the influence of longitudinal ventilation velocity and particle size of water mist on the ceiling temperature, the stable ceiling temperature variation

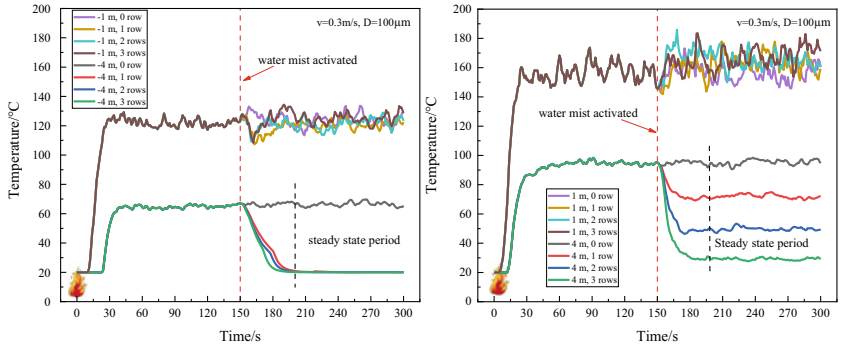

(a) Heat release rate of 31.62kW, upstream (b) Heat release rate of 31.62kW, downstream

(c) Heat release rate of 63.25kW, upstream (d) Heat release rate of 63.25kW, downstream

Fig. 33.3 Ceiling temperature variations on both sides of the water mist screen section in the main tunnel (±1 and ±4 m away from the fire source)

along the downstream of main tunnel with the same number of water mist nozzle rows activated is shown in Fig. 33.5. It can be seen that the variation of wind speed mainly affects the ceiling temperature in the area near the fire source. The higher the wind speed, the lower the ceiling temperature near the fire source. Under the same wind speed, the smaller the particle size of water mist causes the more droplets and the larger specific surface areas, which can obtain the better cooling effect on ceiling temperature in the outside area of the water mist screen section.

Figure 33.6 visually shows the typical temperature flow field distribution in the downstream of main tunnel at 200 s when different number of water mist nozzle rows activated. The influence of the water mist section is strengthened with the increasing rows of water mist nozzles, more smoke are captured and cooled down. Therefore, the ceiling temperature in the area near the fire source increases, while the ceiling temperature in the outside area of the water mist screen section decreases, which is consistent with the previous study by Wang et al. [13].

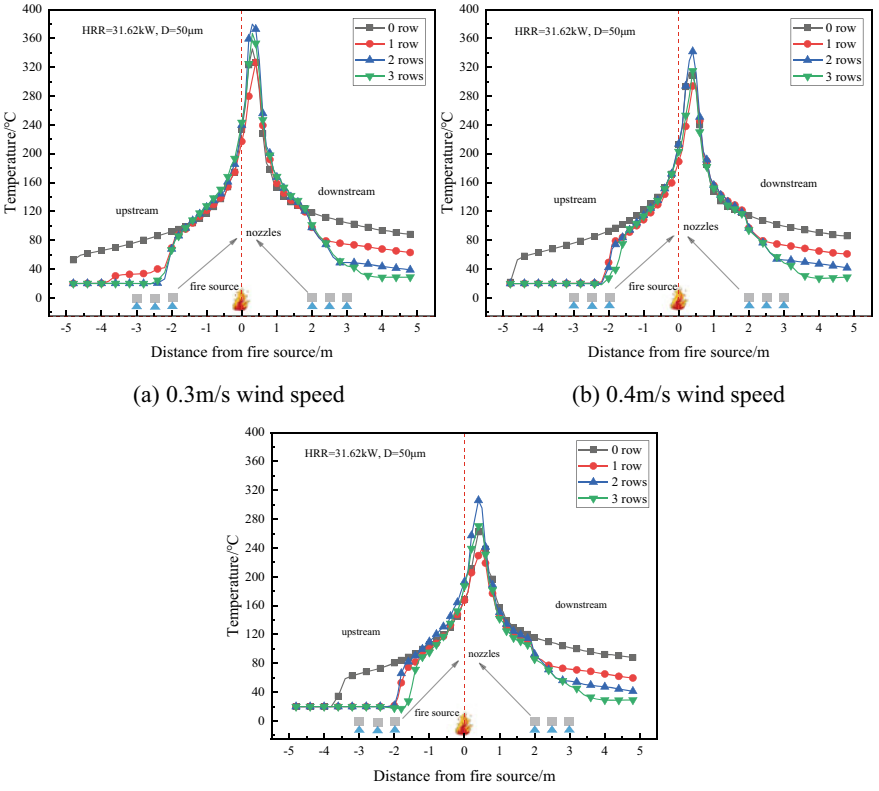

(a) 0.3m/s wind speed

(b) 0.4m/s wind speed

(c) 0.5m/s wind speed

Fig. 33.4 Ceiling temperature along the main tunnel with different water mist nozzle rows

33.3.1.2 CO Concentration

Figure 33.7 shows the ceiling CO concentration distribution along the main tunnel during the stable period. It shows that the water mist screen section has the obvious blocking effect on upstream ceiling CO concentration. When the wind speed is 0.3 m/s, activating 1 row of water mist nozzles can reduce upstream ceiling CO concentration to a certain extent, and the upstream ceiling CO concentration in the outside area of the water mist screen section is basically blocked when 2 rows or 3 rows of water mist nozzles activated. As the wind speed increase to 0.4 and 0.5 m/s, the upstream ceiling CO concentration is completely blocked by water mist screen section in the area near the fire source. It can also be seen that the downstream ceiling CO concentration decreases under the action of water mist screen, and increasing the number of water mist nozzle rows has a better effect on reducing downstream ceiling CO concentration.

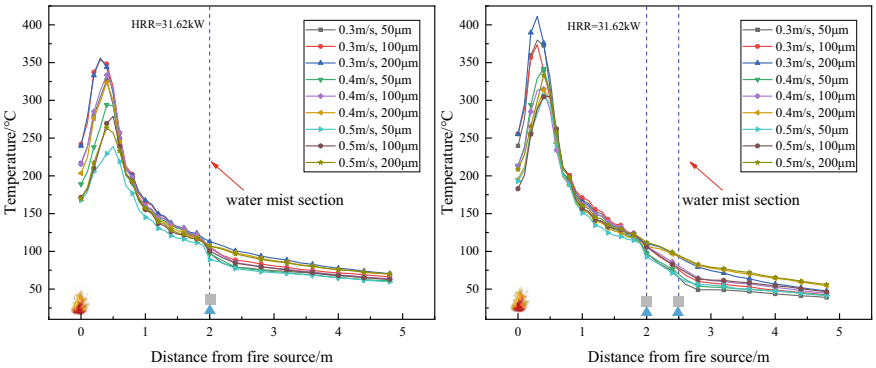

(a) 1 row of water mist nozzles

(b) 2 rows of water mist nozzles

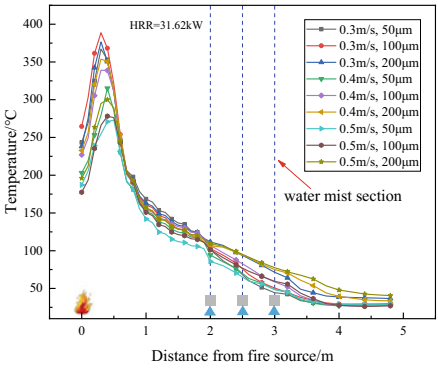

(c) 3 rows of water mist nozzles

Fig. 33.5 Influence of longitudinal ventilation velocity and particle size of water mist on the ceiling temperature along the downstream of main tunnel

The ceiling CO concentration variation with time at 4 m downstream from the fire source of main tunnel is plotted in Fig. 33.8. It can be seen that, the downstream ceiling CO concentration decreases rapidly and remains in a stable fluctuation state after activating the water mist system. When 1 row of water mist nozzles are activated, the smaller the particle size of water mist, the lower the ceiling CO concentration. For all the wind speeds, the particle size of water mist of 200 μm has the worst reducing effect on ceiling CO concentration. The main mechanism of the downward movement of smoke is caused by the drag force from the water droplets [20]. When the 3 rows of water mist nozzles are activated, due to the large amount of droplets, the particle sizes of water mist of 50 and 100 μm have the similar reducing effect on ceiling CO concentration.

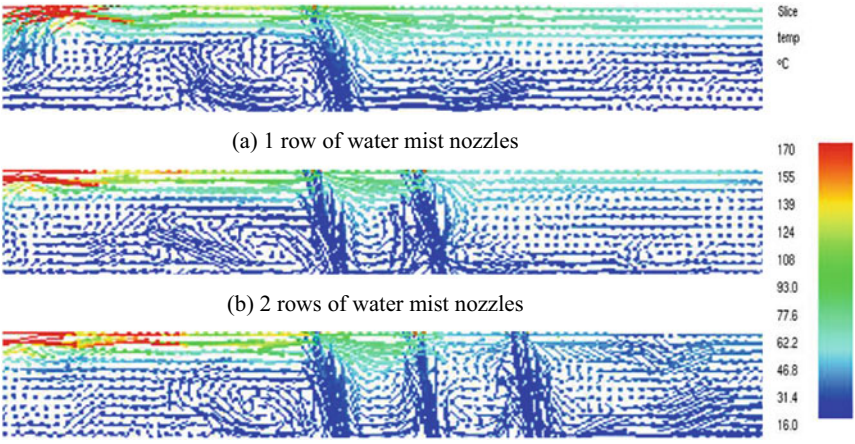

(a) 1 row of water mist nozzles

(b) 2 rows of water mist nozzles

(c) 3 rows of water mist nozzles

Fig. 33.6 Typical temperature flow field distribution in the downstream of main tunnel with different number of water mist nozzle rows activated (t = 200 s)

33.3.2 The Heat Insulation and Smoke Control Effect of the Branch Tunnel

33.3.2.1 Temperature Distribution

According to the above analysis, the coupling effect of longitudinal ventilation and water mist has a significant influence on the upstream ceiling temperature of the main tunnel, but the variation of wind speed has no obvious effect on the downstream ceiling temperature of the main tunnel. It should be noted that due to the bifurcation structure, the wind speed entering the branch tunnel is smaller than the downstream of the main tunnel, so the working condition under the wind speed of 0.5 m/s is selected to analyze the ceiling temperature in the branch.

As shown in Fig. 33.9, under different heat release rates of fire source, the ceiling temperature along the branch tunnel shows a similar variation trend. When there is no water mist, the ceiling temperature along the branch tunnel is exponentially attenuated. After activating the water mist screen, the ceiling temperature drops sharply in the outside region of the water mist section. When 2 rows of water mist nozzles are activated, the ceiling temperature can be reduced to close to the ambient temperature. The cooling effect on ceiling temperature when 3 rows of water mist nozzles activated is almost the same as that of 2 rows.

To verify the influence of particle size of water mist on ceiling temperature, the ceiling temperature variations with time at 3.5 m downstream from the entrance of branch tunnel (i.e., the outside area of the water mist screen section) are compared, as shown in Fig. 33.10. Under the condition that only 1 row of water mist nozzles are activated, the smaller the particle size of water mist results in the lower the

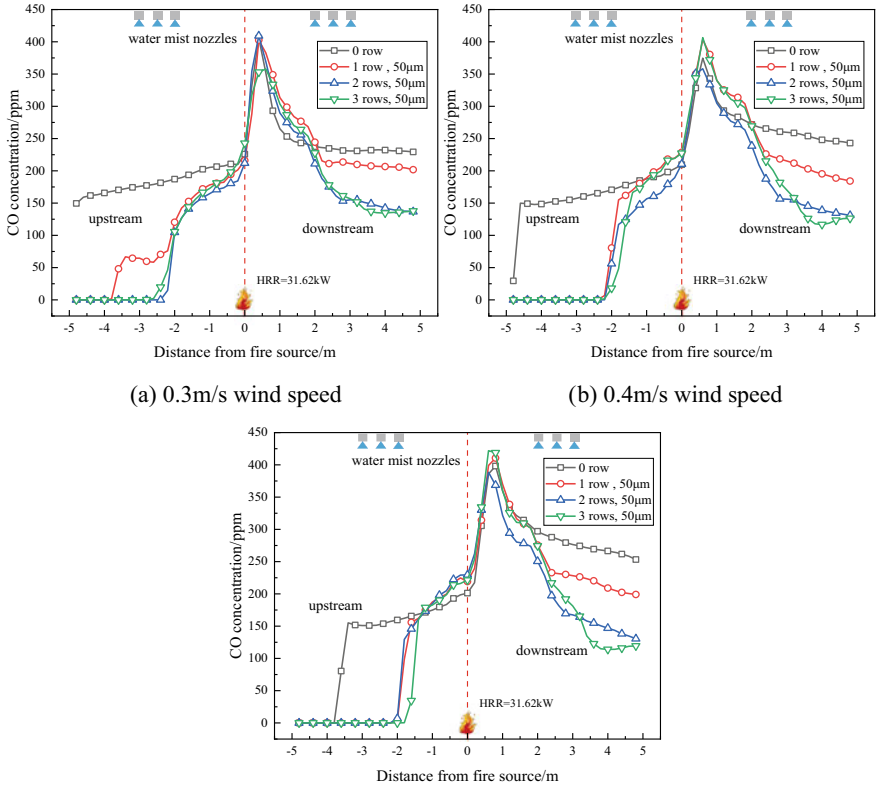

(a) 0.3m/s wind speed (b) 0.4m/s wind speed

(c) 0.5m/s wind speed

Fig. 33.7 Ceiling CO concentration distribution along the main tunnel with different number of water mist nozzle rows activated

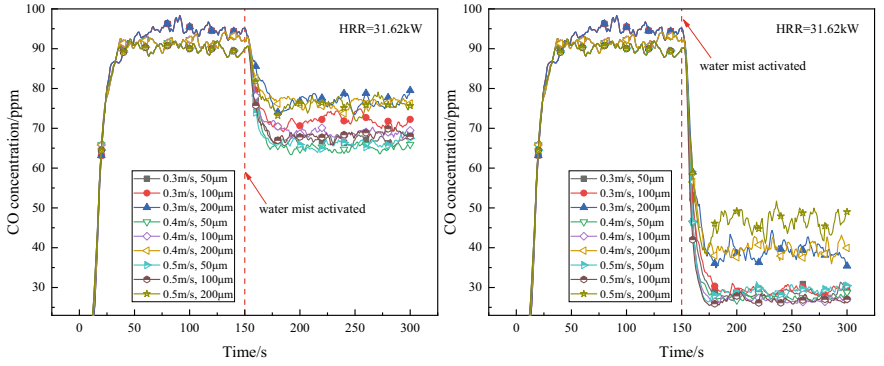

(a) 1 row of water mist nozzles (b) 3 rows of water mist nozzles

Fig. 33.8 Ceiling CO concentration variation with time at 4 m downstream in main tunnel

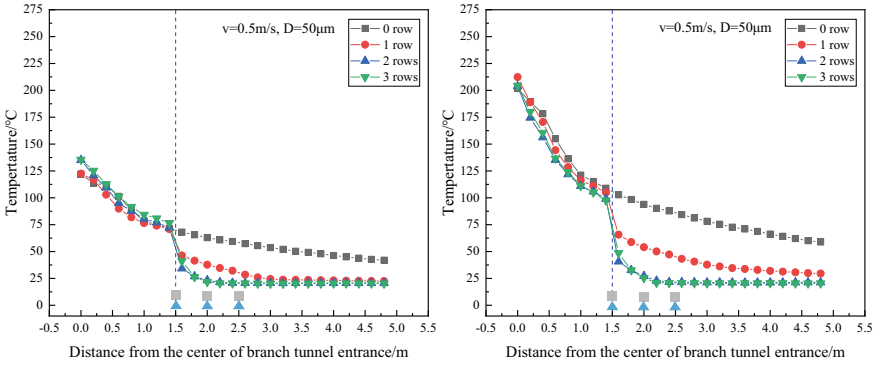

(a) Heat release rate of 31.62kW (b) Heat release rate of 63.25kW

Fig. 33.9 Influence of the number of water mist nozzle rows on ceiling temperature distribution along the branch

ceiling temperature, which further confirms the results obtained in downstream area of the main tunnel. When 2 rows of water mist nozzles are activated, all the three particle sizes of water mist can rapidly reduce the ceiling temperature to the ambient temperature, the cooling effect is already acceptable. At this time, further increasing the number of water mist nozzle rows has no obvious change in the cooling effect on ceiling temperature.

Fig. 33.10 Ceiling temperature variation with time at 3.5 m downstream from the entrance of branch tunnel

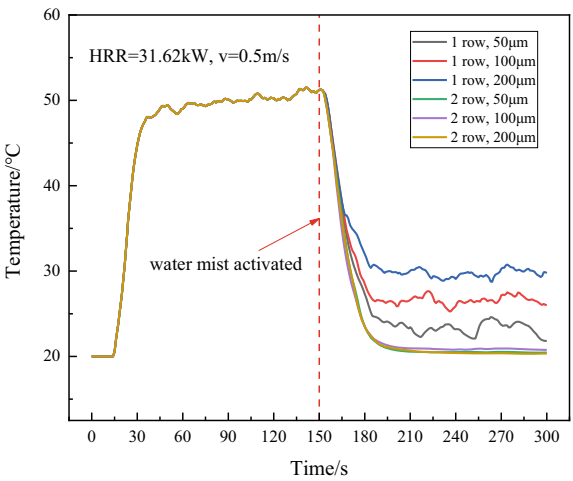

33.3.2.2 CO Concentration

Similar to the ceiling temperature analysis of the branch tunnel, the working condition under the wind speed of 0.5 m/s is selected to analyze the ceiling CO concentration in the branch, seen in Fig. 33.11. After activating the water mist nozzle, the CO concentration near the fire source area increased compared with the original. At the same time, when only one row of nozzles is activated, the farther away from the branch tunnel entrance (i.e., the outside area of the water mist screen section), the more obvious CO concentration decreases along the way. Under this condition, there is little difference in the effect of activating two or three rows of water mist. Activating more nozzles prevents more smoke diffusion than activating a single row of nozzles. As the increase in the number of water mist nozzle rows, the amount of droplets also increases, so more smoke will move downward by the drag force from the droplets, resulting in the better effect on reducing ceiling CO concentration.

To study the influence of particle size of water mist on the ceiling CO concentration, the ceiling CO concentration variation at 1 and 3.5 m downstream from the entrance of branch tunnel with the same number of water mist nozzle rows activated is shown in Fig. 33.12. When only 1 row of water mist nozzles are activated, the three different particle sizes of water mist have the similar blocking effect on ceiling CO concentration. When the particle size was 50 μm, the inhibition effect was better, seen in Fig. 33.12a. As the increase in the number of water mist nozzle rows, reducing effect on ceiling CO concentration of the three particle sizes of water mist begins to differ, and the recovery speed is accelerated. Therefore, compared with the main tunnel, the water mist screen section of branch tunnel has the limited ability to block the smoke diffusion.

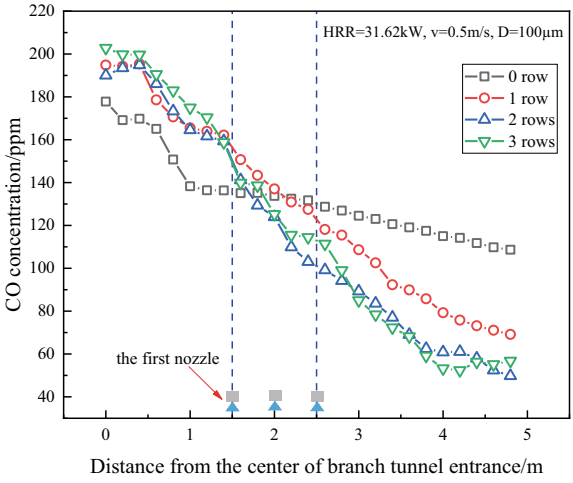

Fig. 33.11 Ceiling CO concentration distribution along the branch tunnel with different number of water mist nozzle rows activated

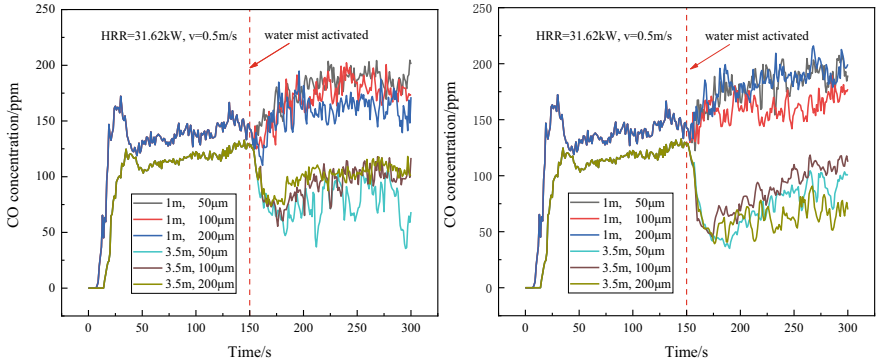

(a) 1 row of water mist nozzles (b) 2 rows of water mist nozzles

Fig. 33.12 Influence of the particle size on the ceiling CO concentration at 1 and 3.5 m downstream from the entrance of branch tunnel

33.4 Conclusions

In this paper, simulation are carried out to study the heat insulation and smoke control effect of water mist screen under the action of longitudinal ventilation in bifurcated tunnel fire. The major conclusions are:

(1) Under the action of water mist system, the longitudinal ventilation has a wonderful cooling effect on the ceiling temperature in the upstream area of main tunnel, but the variation of wind speed has no obvious effect on the downstream ceiling temperature of main tunnel and the ceiling temperature of branch tunnel.

(2) For the ceiling temperature of the main tunnel and branch, the more the number of water mist nozzle rows, the lower the ceiling temperature in the outside area of the water mist screen section, and the better the cooling and heat insulation effect. In general, the smaller particle size also has a better cooling and heat insulation effect.

(3) In the main tunnel, the smaller the particle size of water mist, the lower the ceiling CO concentration. The coupling effect of longitudinal ventilation and water mist on the upstream ceiling CO concentration is obvious, increasing the number of water mist nozzle rows or the wind speed can effectively block the upstream smoke diffusion and reduce the upstream CO concentration. The downstream ceiling CO concentration is less affected by the variation of wind speed, and increasing the number of water mist nozzle rows has a better effect on reducing downstream ceiling CO concentration.

(4) In the branch, due to the influence of the bifurcation structure, the wind speed entering the branch tunnel is smaller and approximates natural ventilation. After activating the water mist system, the ceiling CO concentration decreases firstly and then begins to increase. The more number of water mist nozzle rows results

in the better effect on reducing ceiling concentration. Compared with the main tunnel, the water mist screen section of branch tunnel has the limited ability to block the smoke diffusion.

Acknowledgements This work was supported by the National Key R&D Program of China (Grant No. 2022YFC3801100), and the National Natural Science Foundation of China (NSFC) (Grant No. 51704244).

References

1. Adiga, K.C., Robert, F., Hatcher, J.A.: Computational and experimental study of ultra fine water mist as a total flooding agent. Fire Saf. J. **42**, 150–160 (2007). https://doi.org/10.1016/j.firesaf.2006.08.010
2. White, J.P., Verma, S., Keller, E., Hao, A., Trouve, A., Marshall, A.W.: Water mist suppression of a turbulent line fire. Fire Saf. J. **91**, 705–713 (2017). https://doi.org/10.1016/j.firesaf.2017.03.014
3. Chen, L.Y., Zhu, W., Cai, X., Pan, L.W., Liao, G.X.: Experimental study of water mist fire suppression in tunnels under longitudinal ventilation. Build. Environ. **44**, 446–455 (2008). https://doi.org/10.1016/j.buildenv.2008.04.005
4. Blanchard, E., Boulet, P., Fromy, P., Desanghere, S., Carlotti, P., Vantelon, J., Garo, J.: Experimental and numerical study of the interaction between water mist and fire in an intermediate test tunnel. Fire Technol. **50**, 565–587 (2013). https://doi.org/10.1007/s10694-013-0323-z
5. Li, Q.W., Zhang, P., Guo, S., Pan, P.M., Qin, J., Liao, G.X.: Experimental study on suppression of n-heptane pool fire with water mist under longitudinal ventilation in long and narrow spaces. Procedia Eng. **62**, 946–953 (2013). https://doi.org/10.1016/j.proeng.2013.08.147
6. Wang, J., Xie, Z.C., Lu, K.H., Jiang, X.P., Zhang, H.J.: Water spray flow rate effect on smoke temperature distribution under the ceiling in tunnel fires with longitudinal ventilation. Tunn. Undergr. Space Technol. **79**, 190–196 (2018). https://doi.org/10.1016/j.tust.2018.05.01
7. Yang, Y.B., Yang, B., Bing, Z.: The study on influence of water mist particle size on fire smoke migration with longitudinal ventilation in road tunnel. Procedia Eng. **211**, 917–924 (2018). https://doi.org/10.1016/j.proeng.2017.12.093
8. Li, J., Li, Y.F., Bi, Q., Li, Y., Chow, W.K., Cheng, C.H., To, C.W., Chow, C.L.: Performance evaluation on fixed water-based firefighting system in suppressing large fire in urban tunnels. Tunn. Undergr. Space Technol. **84**, 56–69 (2019). https://doi.org/10.1016/j.tust.2018.10.020
9. Liu, Y.J., Fang, Z., Tang, Z., Beji, T., Merci, B.: The combined effect of a water mist system and longitudinal ventilation on the fire and smoke dynamics in a tunnel. Fire Saf. J. **122**, 103–351 (2021). https://doi.org/10.1016/j.firesaf.2021.103351
10. Magdolenova, P.: CFD modelling of high-pressure water mist system in road tunnels. Transp. Res. Procedia **55**, 1163–1170 (2021). https://doi.org/10.1016/j.trpro.2021.07.184
11. Sun, J.Y., Fang, Z., Tang, Z., Beji, T., Merci, B.: Experimental study of the effectiveness of a water system in blocking fire-induced smoke and heat in reduced-scale tunnel tests. Tunn. Undergr. Space Technol. **56**, 34–44 (2016). https://doi.org/10.1016/j.tust.2016.02.005
12. Liang, Q., Li, Y.F., Li, J.M., Xu, H., Li, K.Y.: Numerical studies on the smoke control by water mist screens with transverse ventilation in tunnel fires. Tunn. Undergr. Space Technol. **64**, 177–183 (2017). https://doi.org/10.1016/j.tust.2017.01.017
13. Wang, J.H., Nie, Q.M., Fang, Z., Tang, Z.: CFD Simulations of the interaction of the water mist zone and tunnel fire smoke in reduced-scale experiments. Procedia Eng. **211**, 726–735 (2018). https://doi.org/10.1016/j.proeng.2017.12.069

14. Li, Q., Tang, Z., Fang, Z., Yuan, J.P., Wang, J.H.: Experimental study of the effectiveness of a water mist segment system in blocking fire-induced smoke and heat in mid-scale tunnel tests. Tunn. Undergr. Space Technol. **88**, 237–249 (2019). https://doi.org/10.1016/j.tust.2019.03.011
15. Mehaddi, R., Collin, A., Boulet, P., Acem, Z., Telassamou, J., Becker, S., Demeurie, F., Morel, J.Y.: Use of a water mist for smoke confinement and radiation shielding in case of fire during tunnel construction. Int. J. Therm. Sci. **148**, 106–156 (2020). https://doi.org/10.1016/j.ijthermalsci.2019.106156
16. Fan, C.G., Bu, R.W., Xie, X.Q., Zhou, Y.: Full-scale experimental study on water mist fire suppression in a railway tunnel rescue station: temperature distribution characteristics. Process. Saf. Environ. Prot. **146**, 396–411 (2021). https://doi.org/10.1016/j.psep.2020.09.019
17. Thomas, P.H.: Modelling of compartment fires. Fire Saf. J. **5**, 181–190 (1983). https://doi.org/10.1016/0379-7112(83)90016-4
18. Tilley, N., Rauwoens, P., Fauconnier, D., Merci, B.: On the extrapolation of CFD results for smoke and heat control in reduced-scale setups to full scale: atrium configuration. Fire Saf. J. **59**, 160–165 (2013). https://doi.org/10.1016/j.firesaf.2013.04.001
19. Drysdale, D.: An Introduction to Fire Dynamics, pp. 132–138. Wiley, United Kingdom (2011)
20. Tang, Z., Fang, Z., Sun, J., Beji, T., Merci, B.: Computational fluid dynamics simulations of the impact of a water spray on a fire-induced smoke layer inside a hood. J. Fire Sci. **36**, 380–405 (2018). https://doi.org/10.1177/0734904118794844